Products from the Reaction of *meso*-Tetrakis(4-halophenyl)porphinatomanganese(II) and Hexacyanobutadiene (HCBD): Formation of π-$[\mathrm{HCBD}]_2^{2-}$ Dimers, μ-$[\mathrm{HCBD}]^{\bullet-}$, σ-$[\mathrm{HCBD}]^{\bullet-}$, and $[\mathrm{C_4(CN)_5O}]^-$

Durrell K. Rittenberg,[a] Ken-ichi Sugiura,[b] Atta M. Arif,[a] Yoshiteru Sakata,[b] Christopher D. Incarvito,[c] Arnold L. Rheingold,[c] and Joel S. Miller*[a]

Dedicated to the memory of Douglas C. Gordon

Abstract: The reaction of hexacyanobutadiene (HCBD) and *meso*-tetrakis(4-chlorophenyl)porphinatomanganese(II) pyridine $[\mathrm{Mn^{II}TClPPpy}]$ (**1Cl**) leads to two phases of $[\mathrm{Mn^{III}TClPPpy}][\mathrm{HCBD}]\cdot\mathrm{PhMe}$ (**α-2Clpy**, **β-2Clpy**). Similarly, the reaction of HCBD and tetrakis(4-bromophenyl)porphinatomanganese(II) pyridine $[\mathrm{Mn^{II}TBrPPpy}]$ (**1Br**) leads to two products $[\mathrm{Mn^{III}TBrPPpy}][\mathrm{HCBD}]\cdot\mathrm{PhMe}$ (**2Brpy**) and $[\mathrm{Mn^{III}TBrPP}][\mathrm{HCBD}]\cdot 2\,\mathrm{PhMe}$ (**3Br**). The structure of dark-green **α-2Clpy** consists of one porphyrin unit with $\mathrm{Mn^{III}}$ in a square pyramidal coordination environment axially bound to one pyridine. The cation forms $[\mathrm{Mn^{III}TClPPpy}]_2^{2+}$ as cofacial dimerized porphyrins. Each $[\mathrm{HCBD}]^{\bullet-}$ is nonplanar with a torsion angle of 170.8(4)° about the center C−C bound, and forms $[\mathrm{HCBD}]_2^{2-}$ dimers in the solid state with sub-van der Waals contacts of 3.325 and 3.340 Å. The magnetic data above 10 K obey the Curie–Weiss expression with a θ of -2.5 K, and μ_{eff} (300 K) $= 4.91\,\mu_{\mathrm{B}}$ as expected for $S = 2\,\mathrm{Mn^{III}}$ and $S = 0$ $[\mathrm{HCBD}]_2^{2-}$. The magnetic data for **α-2Clpy** can be fit with an zero-field-splitting D of -1.45 K. **β-2Clpy** consists of one porphyrin unit with $\mathrm{Mn^{III}}$ in a distorted octahedral coordination environment axially bound to py and to a monodentate $[\mathrm{HCBD}]^{\bullet-}$ bound via an *exo*-nitrile. $[\mathrm{HCBD}]^{\bullet-}$ is nonplanar with a torsion angle of 169.7(5)° about the center C−C bound. The μ_{eff} (350 K) is $5.09\,\mu_{\mathrm{B}}$; however, the magnetic data do not obey the Curie–Weiss expression above 70 K. The low temperature data may be fit with a θ of -5.4 K. The data was modeled to an isolated $S = 2$ and $S = ½$ dinuclear spin system with $J/k_{\mathrm{B}} = -90$ K. Decomposition of $[\mathrm{HCBD}]^{\bullet-}$ to $[\mathrm{C_4(CN)_5O}]^-$ was evidenced by the determination of the structure of $[\mathrm{Mn^{III}TClPP}][\mathrm{C_4(CN)_5O}]\cdot 2\,\mathrm{PhMe}$ (**3Cl-O**). Crystals of **3Cl-O** were prepared by reaction of HCBD and **1Cl** in the presence of a drop of water. The molecular structure consists of $[\mathrm{HCBD}]^{\bullet-}$ *trans*-μ-*N*-2,3-bound to $[\mathrm{Mn^{III}TBrPP}]^+$ forming a 1-D coordination polymer of alternating $[\mathrm{Mn^{III}TBrPP}]^+$ and $[\mathrm{HCBD}]^{\bullet-}$. The intrachain Mn···Mn distance was 10.675(3) Å, with important interchain Mn···Mn distances of 10.832, 11.016, and 14.696 Å. The magnetic data were fit to a Curie–Weiss law ($10 < T < 290$ K) with a θ of -3.5 K, and $D = 0.3$ K with $\mu_{\mathrm{eff}} = 4.97\,\mu_{\mathrm{B}}$ at 300 K.

Keywords: electron transfer · magnetic properties · metalloporphyrins · polymers

Introduction

The discovery of bulk magnetic ordering in $[\mathrm{MnTPP}]^+[\mathrm{TCNE}]^{\bullet-}\cdot 2\,\mathrm{PhMe}$ ($\mathrm{H_2TPP}$ = *meso*-tetraphenylporphyrin, TCNE = tetracyanoethylene) below its magnetic ordering temperature T_{c} of 15 K[1] has led to a family of related magnets.[2] One aspect of current research focuses on exploring other organic acceptors with substituted *tetra*-phenylporphyrins to establish relationships between the structure and the magnetic phenomena, particularly in the correlation of dimensionality, connectivity, and the critical temperature of this class material.

Hexacyanobutadiene (HCBD) is a strong organic acceptor[3a] ($E^0 = 0.60$ eV vs. SCE),[3b] that forms 1-D $\cdots\mathrm{D^+A^{\bullet-}D^+A^{\bullet-}}\cdots$ chains with metallomacrocycles binding in two motifs either *trans*-μ-*endo*-*N*-σ-bound (***A***) exemplified by $[\mathrm{Mn^{III}OEP}][\mathrm{HCBD}]$ ($\mathrm{H_2OEP}$ = octaethylporphyrin)[4] or *trans*-μ-2,3-*N*-σ-bound (***B***) exemplified by $[\mathrm{Mn^{III}T}t\mathrm{BuPP}][\mathrm{HCBD}]$ ($\mathrm{H_2T}t\mathrm{BuPP}$ = *meso*-tetrakis(4-tetrabutylphenyl)porphyrin).[5] The complexes exhibit very different magnetic couplings ascribed to the differences in the spin density located on the *endo* (***A***) and interior (***B***) nitrogens.

---

[a] Prof. J. S. Miller, Dr. D. K. Rittenberg, Dr. A. M. Arif
Department of Chemistry
University of Utah, Salt Lake City, UT 84112 (USA)
Fax: (+1) 801 581 8433
E-mail: jsmiller@chemistry.utah.edu

[b] Dr. K.-i. Sugiura, Prof. Y. Sakata
Osaka University
Institute for Industrial and Scientific Research
Osaka, 565 (Japan)
Fax: (+81) 6 87 8479
E-mail: Sugiura@sanken.osaka-u.ac.jp

[c] C. D. Incarvito, Prof. A. L. Rheingold
Department of Chemistry
University of Delaware, Newark, DE 19716 (USA)
Fax: (+1) 302 831 6335
E-mail: arnrhein@udel.edu

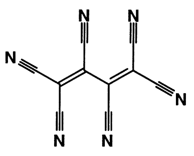

HCBD

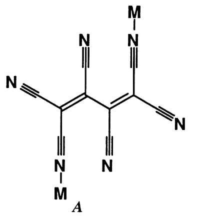

A

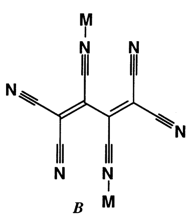

B

As a result, the spin overlap describing the coupling is substantially diminished for interior-bound [HCBD]$^{\bullet-}$, in accord with the low θ value obtained from a fit of the magnetic susceptibility to the Curie–Weiss expression of -15 K for [MnT*t*BuPP][HCBD],[5] and a substantially higher θ value of 67 K for [MnOEP][HCBD].[4] Due to the ease of modifying the porphyrin structure, we are studying electron-transfer salts of substituted-Mn^{II}TPP complexes with HCBD to identify factors responsible for differences in [HCBD]$^{\bullet-}$ binding and subsequent magnetic coupling. Herein, we report the structural, chemical, magnetic, and thermal properties of several HCBD electron transfer salts with *meso*-tetrakis(4-chlorophenyl)porphinatomanganese(II) pyridine [Mn^{II}TClPPpy] (**1Clpy**), and *meso*-tetrakis(4-bromophenyl)-porphinatomanganese(II) pyridine [Mn^{II}TBrPPpy] (**1Br**).

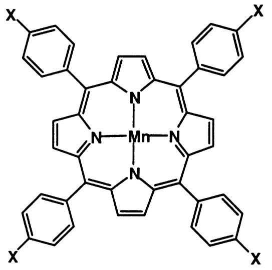

1Cl (X = Cl), Mn^{II}TClPPpy

1Br (X = Br), Mn^{II}TBrPPpy

Results and Discussion

The reaction of [Mn^{II}TXPPpy] [X = Cl (**1Cl**), Br (**1Br**)] and HCBD leads to the isolation of dark green ***α*-2Clpy**, ***β*-2Clpy**, and **2Brpy**, after 2 d. $\tilde{\nu}_{CN}$ absorptions of 2185 (m), 2170 (s), and 2128 (m) cm^{-1} occur for ***α*-2Clpy**, and 2185 (m), 2170 (s), 2153 (m) cm^{-1} for both ***β*-2Clpy** and **2Brpy**. These $\tilde{\nu}_{CN}$ IR absorptions are consistent with each other and other known [HCBD]$^{\bullet-}$ salts that range from 2150 to 2230 cm^{-1},[6, 7] but are inconsistent with either [HCBD]$^{2-}$ (2120 to 2200 cm^{-1}) or HCBD (2210 to 2250 cm^{-1}).[7] Nonetheless, these values are inconsistent both unbound [HCBD]$^{\bullet-}$, such as [FeCp*$_2$][HCBD] (Cp* = pentamethylcyclo-pentadienide) [2185 (s) and 2168 (m) cm^{-1}],[8] or either mode of *trans-N*-σ-bound [HCBD]$^{\bullet-}$ (***A*** or ***B***).[4, 5] The $\tilde{\nu}_{CN}$ for ***α*-2Clpy** is inconsistent with known [HCBD]$^{\bullet-}$ complexes.[6, 7] The 2128 cm^{-1} absorption suggests a new structural arrangement for reduced HCBD.

When the reaction mixture of **2Brpy** is left standing for about three weeks a block-crystal product, **3Br**, is isolated. The $\tilde{\nu}_{CN}$ absorptions for **3Br** are 2228 (m), 2212 (s), and 2189 (m) cm^{-1}.[9] These absorptions appear at significantly higher frequency than **2Clpy** and **2Brpy**, but are within the range of known bound [HCBD]$^{\bullet-}$ anions.[6, 7]

Thermogravimetric analysis coupled with mass spectroscopy (TGA/MS) studies reveal weight losses of ~14.5% for ***α***- and ***β*-2Clpy** and 18.9% for **2Brpy** in accord with the loss of one toluene and one pyridine in the former (calcd 14.6%) and two toluenes and one pyridine in the latter (calcd 19.0%). The TGA/MS spectrum of **3Br** shows a weight loss between 100 and 180 °C of 14.0% (calcd 14.0%), due to the loss of 2.10 toluene with no evidence of pyridine in the mass spectrum.

Attempts to grow single crystals of **3Cl** upon long standing led to isolation of a fourth product characterized as [Mn^{III}TClPP][C$_4$(CN)$_5$O]·2PhMe (**3Cl-O**). As with [TCNE]$^{\bullet-}$,[10] [HCBD]$^{\bullet-[3a]}$ is unstable in aerobic and aqueous environments, and can decompose to [OC(CN)C(CN)-C(CN)C(CN)$_2$]$^-$. Although the structures of several tricyanoethenolate coordination complexes have been reported,[10] this is the first reported structure of the pentacyanobutadienolate anion. The presence of [C$_4$(CN)$_5$O]$^-$ can be ascertained from the IR spectra which exhibits distinct $\tilde{\nu}_{CN}$ absorptions of 2235 (w) (sh), 2226 (m), and 2218 (m) cm^{-1} and $\tilde{\nu}_{CO}$ 1557 (s) cm^{-1} in accord with 2219 (m), 2196 (w), and 1558 (s) cm^{-1} $\tilde{\nu}_{CN}$ absorptions for [MnTOMePP][C$_2$(CN)$_3$O].[10]

Complex **3Br** can also be prepared directly by using excess HCBD rather than a stoichiometric mixture, or by replacing pyridine with weaker coordinating 2-methylpyridine and 2,6-dimethylpyridine ligands in the Mn^{II}TXPP starting material. In both cases a black precipitate is isolated in 24 h with its characteristic IR absorptions.

Crystal structures: ***α*-2Clpy** is composed of one [Mn^{III}TClPPpy]$^+$, D, one [HCBD]$^{\bullet-}$, A, and one toluene solvate per repeat unit (Figure 1). Each Mn^{III} is surrounded by five nitrogen atoms (four porphyrinic and one from pyridine) in a distorted square pyramidal geometry with Mn–N$_{pyrrole}$ bond distances averaging 2.007 Å and a Mn–N$_{pyridine}$ distance of 2.316(8) Å. The porphyrin macrocycle is significantly distorted adopting a saddle conformation. Furthermore, the Mn is displaced from the mean pyrrole-N$_4$ plane by 0.53 Å. This nonplanar geometry has also been observed several TPP derivatives,[11] such as [MnTPP][C$_3$(CN)$_5$].[11c] The bond distances and angles of the [HCBD]$^{\bullet-}$ are summarized in Table 1. The C–C bond distances for the C$_4$ backbone range from 1.384(6) to 1.402(6) Å averaging 1.391(6) Å in good agreement with predicted values for bond order of 1.5 expected for [HCBD]$^{\bullet-}$.[7] The C–CN bond distances for the *exo*-, *endo*- and interior position range from 1.410(6) to 1.464(5) Å averaging 1.422 Å. These data are in good agreement with [MnT*t*BuPP][HCBD] (1.445 Å)[5] and [MnOEP][HCBD] (1.433 Å).[4] These data are less than that found for either with [MnT*t*BuPP][HCBD] (1.445 Å)[5] or [MnOEP][HCBD] (1.433 Å).[4] The CN bond distances for the *exo*-, *endo*- and interior positions range from 1.139(5) to 1.167(5), and average 1.156 Å. The N-C-C bond angles average 175.1°, whereas the NC-C-C bond angles average 121.2°. The most surprising structural feature of [HCBD]$^{\bullet-}$ is the pronounced torsion angle along the C$_4$ backbone of 170.8(4)°. Previously, the reported structure of described a

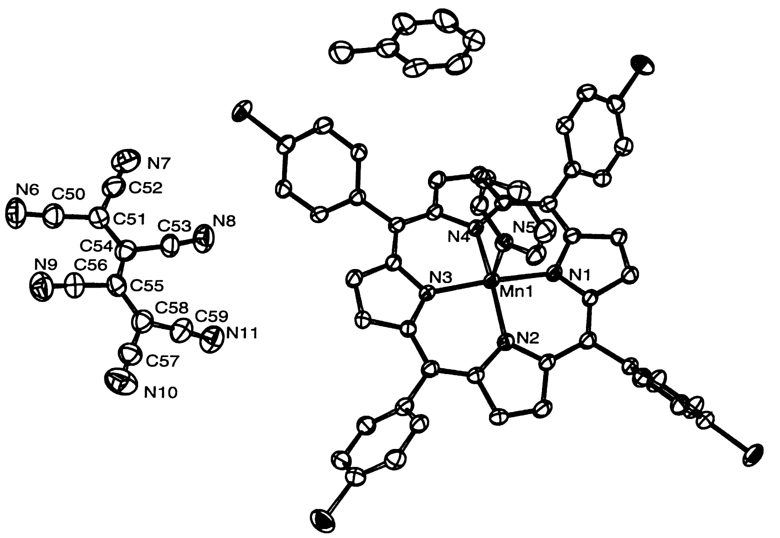

Figure 1. ORTEP diagram drawn at 30% probability of α-[MnTClPPpy][HCBD]·PhMe (**α-2Clpy**).

twisted conformation; however, the twist was much more pronounced (40°) then the present case.[7]

The structure of **α-2Clpy** consists of cofacial π-$[Mn^{III}TClPPpy]_2^{2+}$ cations separated by π $[HCBD]_2^{2-}$ dimers (Figure 2). The cofacial π-$[Mn^{III}TClPPpy]^+$ intradimer separation is 4.10, while the Mn–Mn separation is 5.41 Å. The $[HCBD]_2^{2-}$ intradimer separation ranges from 3.325 to 3.401 Å. Although there are a number of cofacial π porphyrin dimers,[12] this is the first example of a dimerized $[HCBD]_2^{2-}$. Several HCBD electron transfer salts have been characterized crystallographically.[6] Generally $[HCBD]^{\bullet -}$ is isolated as observed for [TMTTF][HCBD][13a] (TMTTF = tetramethyltetrathiafulvalene) and $[Fe(C_5Me_5)_2][HCBD]$,[8] but may bridge two metal sites, as observed for [MnOEP][HCBD][4] and $[Mn^{III}T\textit{t}BuPP][HCBD]$.[5] The π overlap present for $[HCBD]_2^{2-}$ is limited to ⅓ of the $[HCBD]^{\bullet -}$ ion, the $C_2(CN)_3$ moiety, and may be the origin of the deviation form the mean plane observed in the C_4 backbone. Hence, $[HCBD]_2^{2-}$ is neither eclipsed like previously reported for several $[TCNE]_2^{2-}$ complexes,[14] nor slipped as observed for $[TCNQ]_2^{2-}$ (TCNQ = 7,7,8,8-tetracyano-*p*-quinodimethane) dimers.[15] The closest π-$[HCBD]_2^{2-}$ contact is 3.325 Å between N(10) and C(54) with other close contacts averaging 3.340 Å. The observed intradimer distances are consistent with other dimerized cyanocarbons, for example the α- and β-phase of [TTF][TCNE][14a] (TTF = tetrathiafulvalene) which exhibit intradimer distances of 3.39 and 3.26 Å, respectively, but longer than those found in $Cu(PPh_3)TCNE$[14b] (3.149 Å) or $[Cr(C_6H_6)_2][TCNE]$[14c] (3.09 Å). Preliminary ab initio calculations at the UHF level suggest a singlet ground state with a singlet–triplet energy gap is ~65 kcal mol^{-1}[16] consistent with no contribution to the magnetic moment (vide infra).

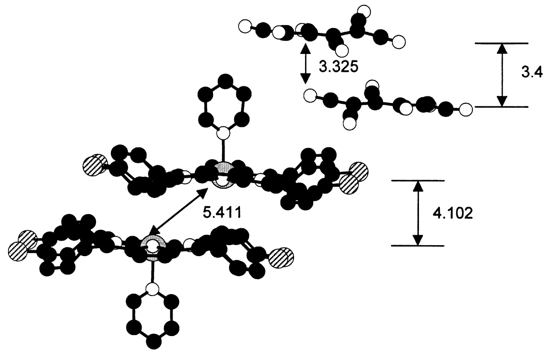

Figure 2. Molecular structure of α-[MnTClPPpy][HCBD]·PhMe (**α-2Clpy**) and dimer stacking arrangement. The solvent and hydrogen atoms have been removed for clarity.

β-2Clpy, like **α-2Clpy**, is comprised of $[Mn^{III}TClPPpy]^+$-$[HCBD]^{\bullet -}$, and one toluene solvate (Figure 3). A slight rotational disorder was observed in the toluene solvate and was subsequently modeled as a flat hexagon. Unlike for **α-2Clpy**, the Mn^{III} occupies a distorted octahedral coordination

Table 1. Summary of the bond distances, Å, and bond angles of the $[HCBD]^{\bullet -}$.

α-2Cl		**β-2Cl**		**3Br**		**3Cl-O**	
Mn(1)–N(5)	1.992(7)	Mn(1)–N(5)	1.993(4)	Mn(1)–N(1)	2.009(3)	Mn(1)–N(1)	2.033(6)
Mn(1)–N(4)	2.003(7)	Mn(1)–N(4)	2.004(4)	Mn(1)–N(2)	2.004(3)	Mn(2)–N(4)	2.023(7)
Mn(1)-N(1)	2.316(8)	Mn(1)–N(11) (Py)	2.281(4)	Mn(1)–N(5)HCBD	2.216(3)	Mn(1)–N(300)	2.315(6)
		Mn(1)–N(1) (HCBD)	2.506(5)			Mn(2)-O(1)	2.279(5)
N(1)–C(1)	1.131(13)	N(1)–C(1)	1.152(8)	N(8)–C(53)	1.160(5)	N(302)-C(303)	–
		N(2)–C(7)	1.138(1)	N(9)–C(56)	1.167(5)	N(300)–C(300)	1.141(10)
N(2)-C(4)	1.02(2)	N(3)–C(8)	1.128(8)	N(6)–C(50)	1.143(5)	N(303)–C(302)	1.149(5)
		N(4)–C(9)	1.137(10)	N(11)–C(59)	1.139(5)	N(301)–C(301)	1.30(1)
N(3)–C(5)	1.072(14)	N(5)–C(6)	1.127(12)	N(7)-C(52)	1.164(5)	N(304)–C(305)	1.157(11)
		N(6)–C(10)	1.146(10)	N(10)-C(57)	1.157(5)		
C(1)–C(2)	1.510(19)	C(2)–C(3)	1.442(10)	C(53)–C(54)	1.459(5)	C(303)–C(307)	1.46(1)
		C(4)–C(5)	1.418(10)	C(56)–C(55)	1.464(5)	C(300)–C(308)	1.41(1)
C(2)–C(2′)	1.39(2)	C(3)–C(4)	1.378(10)	C(54)–C(55)	1.386(5)	C(307)–C(308)	1.42(1)
C(2)–C(3)	1.20(2)	C(1)–C(2)	1.415(9)	C(54)–C(51)	1.402(6)	C(304)–C(308)	1.405(10)
		C(3)–C(8)	1.453(8)	C(55)-C(58)	1.384(6)	C(306)–C(307)	1.383(13)

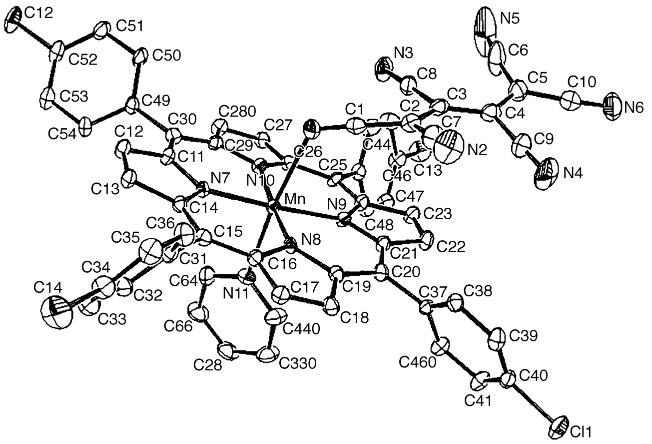

Figure 3. ORTEP diagram drawn at 30% probability of *β*-[MnTClPPpy][HCBD]·PhMe (***β*-2Cl**). Hydrogen atoms and toluene solvate have been omitted for clarity.

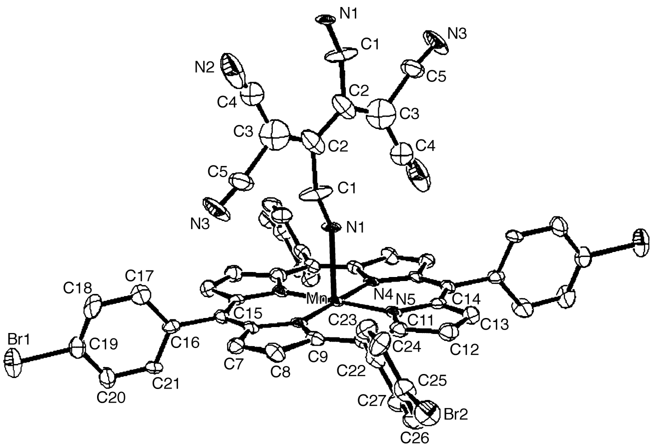

Figure 4. ORTEP diagram drawn at 30% probability of [MnTBrPP][HCBD]·2PhMe (**3Br**). Hydrogen atoms and toluene solvate have been omitted for clarity.

environment with pyridine and [HCBD]$^{\bullet -}$ occupying axial coordination sites. Mn–N$_{\text{porphyrin}}$ distance average 2.000 Å, with the other bond angles and distances being typical of [Mn$^{\text{III}}$TPP]$^+$ cations (see Table 1).[1, 2, 10, 11, 17] The Mn–N$_{\text{HCBD}}$ bond distance of 2.506 Å is significantly longer than those for [MnOEP][HCBD] (2.419 Å),[4] [Mn$^{\text{III}}$T*t*BuPP][HCBD] (2.306 Å), and [MnTPP][TCNE] complexes.[5] On the other hand, the Mn–N$_{\text{py}}$ bond distance of ***β*-2Clpy** is 2.281 Å, significantly shorter than the Mn–N$_{\text{HCBD}}$ distance, but close to the Mn–N$_{\text{py}}$ distance of ***α*-2Clpy** (2.216 Å). The [HCBD]$^{\bullet -}$ anion is significantly twisted with a center C_4 backbone dihedral angle of 169.7° in agreement with ***α*-2Clpy** (170.8°). Unlike previous [MnTPP][HCBD] complexes that coordinate to interior nitriles, ***β*-2Clpy** binds to the *exo*-nitrile. Furthermore, in addition to the long Mn–N distance, the 121.1° Mn-N-C bond angle suggests dominate sp^2 bonding interaction is through the lone pair on nitrogen, **4**, whereas in [HCBD]$^{\bullet -}$ chain complexes of MnTPP derivative bond angles approach 180°, which suggests a π-type bonding mode.

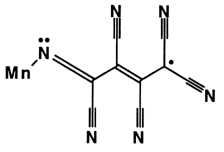

4

The packing motif of ***β*-2Clpy** consists of parallel chains of [MnTClPPpy][HCBD] along *c*. Due to this stacking arrangement porphyrin units stack such that the [HCBD]$^{\bullet -}$ are on opposite sides of each porphyrin. These chains are separated by toluene solvates. No close contacts were observed in the crystal lattice, and intermolecular Mn···Mn distances were mostly of 9.0 Å.

Complex **3Br** has one-half of an ordered [Mn$^{\text{III}}$TBrPP]$^+$, one-half of a disordered [HCBD]$^{\bullet -}$, and an ordered toluene solvate where the cation and anion occupy special positions (center of inversion) in the unit cell with an ordered toluene (Figure 4). The [HCBD]$^{\bullet -}$ disorder could not be resolved; however, it is believed to be rotationally disordered along C_4backbone as observed for [FeCp*$_2$][HCBD][8] and [TMTTF][HCBD].[13] The average Mn–N$_{\text{pyrrole}}$ bond distance is 2.007 Å, while the Mn–NC$_4$ bond distance is 2.316(8) Å, typical for this class of materials. [HCBD]$^{\bullet -}$ is planar with an average C–C bond distance for the C_4 backbone of 1.26 Å; however, due to disorder this value is not useful for comparison. The C–CN bond distances average 1.53 Å, while the C–CN-Mn bond distance is 1.51(2) Å. The C≡N and C≡NMn distances are 1.046 Å and 1.131 Å, which are significantly shorter than that observed for [MnT*t*BuPP][HCBD].[5] Complex **3Br** is comprised of 1-D···D$^+$A$^{\bullet -}$D$^+$A$^{\bullet -}$··· chains in which the [HCBD]$^{\bullet -}$ is *trans*-interior-*μ*-*N*-σ-bound to Mn with a typical Mn–NC bond distance of 2.316(8) Å (Figure 5). The Mn-N-C 160.0(10)° angle is midway between that of [MnT*t*BuPP][HCBD][5] (172.3°), and [MnOEP][HCBD] (148.1°) which has different bonding motif.[4] The dihedral angle between the MnN$_4$ plane and plane of one half of [HCBD]$^{\bullet -}$ is 83.7(3)° close to that found for [MnT*t*BuPP][HCBD] (87.4°).[5] In the structurally related [MnTPP][TCNE] family of magnets, it has been shown that

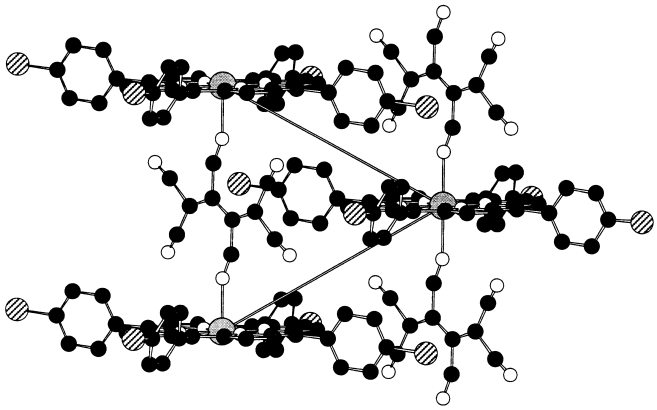

Figure 5. Segment of a 1-D ···D$^+$A$^{\bullet -}$D$^+$A$^{\bullet -}$··· chain showing interior *trans*-*μ*-*N*-*σ*-binding of [HCBD]$^{\bullet -}$ to [MnTBrPP]$^+$ in [MnTBrPP][HCBD]·2PhMe (**3Br**) and important interchain interactions.

this angle is inversely proportional to the strength of the 1-D antiferromagnetic coupling between the Mn^{III} and $[TCNE]^{\bullet -}$.[18] Smaller MnN_4-$[TCNE]^{\bullet -}$ dihedral angles led to stronger 1-D coupling due to increased σ-overlap of the spin containing p_z orbital on $[TCNE]^{\bullet -}$ with the $d_z{}^2$ orbital on Mn^{III}.[18] It was hoped a similar correlation could be realized for the [MnTPP][HCBD] family; however, more structurally related examples are needed before such a correlation can be established. The intrachain Mn⋯Mn separation is 10.657 Å, identical to that observed for [MnT*t*BuPP][HCBD] (10.652 Å),[5] but shorter than the 10.844 Å observed for [MnOEP][HCBD].[4] However, the observed interchain separations for **3Br** are 10.832 and 11.016 Å significantly shorter than 16.522 and 16.034 Å for the [MnT*t*BuPP][HCBD].[5]

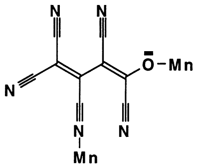

5

$[MnTClPP][C_4(CN)_5O]\cdot 2PhMe$ (**3Cl-O**) is composed of one half of two separate $[Mn^{III}TClPP]^+$ units bridged by a pentacyanobutadienolate $[C_4(CN)_5O]^-$ anion bound to Mn1 via the internal nitrile and Mn2 by oxygen, **5** (Figure 6). The Mn–N and Mn–O bond distances are 2.315 (6) and 2.279 (9) Å, respectively, compared with 2.326 Å for Mn–N/O for the similar 1-D, albeit disordered, chained tricyanoethenolate $[MnTOMePP][C_2(CN)_3O]$.[10] The $Mn1-N_{ring}$ and $Mn2-N_{ring}$ bond distances average 2.022 and 2.005 Å, respectively, with other cation bond distances and angles typical of $[Mn^{III}TPP]^+$.[1, 2, 10, 11, 18] The coordination environment of Mn1 consists of a nitrogen bound axially distorted octahedron. Whereas Mn2 occupies an axially distorted octahedral with an intrachain Mn⋯Mn separation of 8.601 Å and interchain Mn⋯Mn separations ranging from 13.830 to 17.287 Å. This is the first reported structure of the $[C_4(CN)_5O]^-$ anion. Interestingly, coordination of the nitrile occurs though an interior N as for **3Br** (Figure 7), rather than the *endo*- or *exo*-position as observed in [MnOEP][HCBD][4] or ***β*-2Cl**. The Mn(1)-O-C and Mn(2)-N(300)-C(300) bond angles are 121.1 and 169.3°, respectively, which suggests that the oxygen is bound through the lone pair and as with **3Br** the nitrile bonding is π-like.

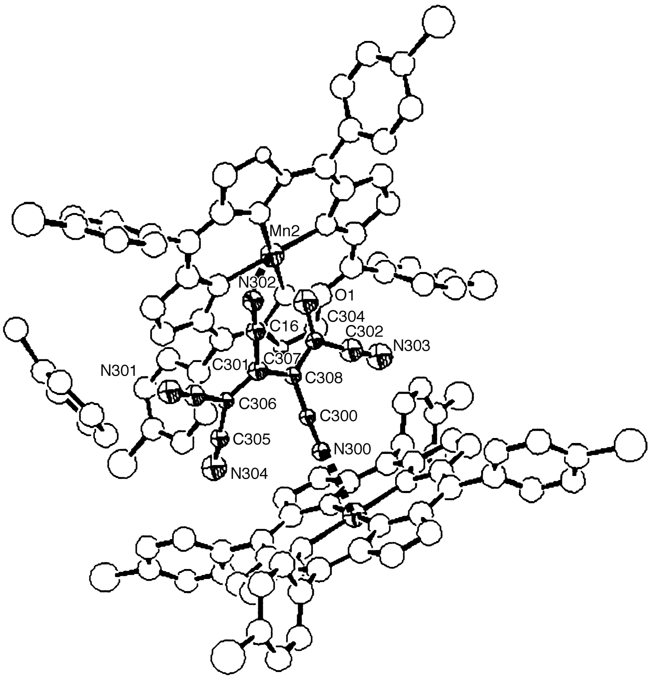

Figure 6. ORTEP diagram drawn at 30% probability of $[MnTClPP][C_4(CN)_5O]\cdot 2PhMe$ (**3Cl-C$_4$(CN)$_5$O**). Hydrogen atoms and toluene solvate have been omitted for clarity.

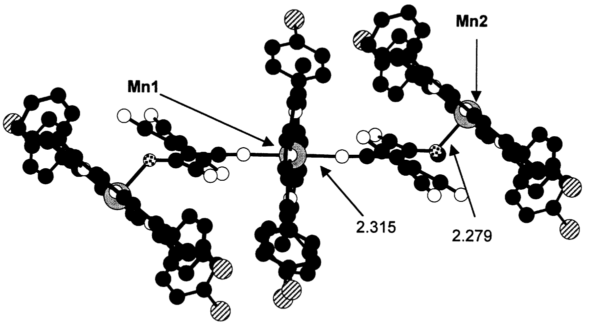

Figure 7. Segment of a 1-D $\cdots D^+A^{\bullet -}D^+A^{\bullet -}\cdots$ chain showing $[C_4(CN)_5O]^-$ to $[MnTClPP]^+$ in $[MnTClPP][C_4(CN)_5O]\cdot 2PhMe$ (**3Cl-O**).

Magnetic properties: The 5 to 300 K temperature dependence of the magnetic susceptibility χ of ***α*-2Clpy**, ***β*-2Clpy**, and **3Br** were studied. The data for ***α*-** and ***β*-2Clpy** can be fit to a Curie–Weiss expression $\chi \propto 1/(T-\theta)$ between 10 to 300 K and 5 to 140 K with θ of −2.5 and −6.6 K, respectively (Figure 8). In both cases the magnitude of the observed θ, $|\theta|$, is significantly lower than that of [MnT*t*BuPP][HCBD], −15 K,[5] or [MnOEP][HCBD], 67 K,[4] which suggests attenuated magnetic coupling. The 300 K effective moment, $\mu_{eff} = (8\chi T)^{1/2}$, for ***α*-** and ***β*-2Clpy** are 4.91 and 4.88 μ_B, respectively. For ***α*-2Clpy** the 4.91 μ_B value is as expected for $S = 2$ and $g = 2$ system; hence, no contribution from $[HCBD]_2{}^{2-}$ is evident. Thus, the effective moment of ***α*-2Clpy** strongly suggests a singlet ground state of the $[HCBD]_2{}^{2-}$. Nonetheless, given the long intradimer separation, thermal population of the triplet excited state might be achieved; however, no evidence of such a transition was observed below a temperature of 400 K. Likewise, evidence of long range magnetic ordering was not observed in either sample.

The temperature dependence of μ_{eff} for ***α*-2Clpy** can be fit to an expression for zero-field-splitting ($H = DS_z{}^2 + g\mu_B\mathbf{H}\cdot\mathbf{S}$), Equation (1),[19] with $S = 2$, $g = 1.99$ and zero-field-splitting parameter D of −1.45 K (−2.09 cm^{-1}).

$$\mu^2 = \frac{2g^2\,(e^{-D/T} + 4\,e^{-D/T})}{1 + 2\,e^{-D/T} + 2\,e^{-4D/T}} + \frac{2g^2\,(18 - 14\,e^{-D/T} + 4\,e^{4-D/T})}{3D\,(1 + 2\,e^{-D/T} + 2\,e^{4-D/T})} \tag{1}$$

For typical five- and six-coordinate $[Mn^{III}TPP]^+$-containing complexes D ranges between −2.6 and −4.3 K.[20] The reduced value in the present case is likely due to the distorted porphyrin moiety changing the coordination environment about Mn. The slope observed in $\mu_{eff}(T)$ with increasing temperature is indicative of temperature independent paramagnetism TIP.[21] Subsequently the best fit to the data was obtained with the addition of a TIP term of 200 × 10^{-6} emu mol^{-1} (Figure 8). Typically, Mn^{III} does not exhibit TIP; however, in the present case the coordination environment of the Mn center is significantly distorted and maybe the origin of the observed behavior.

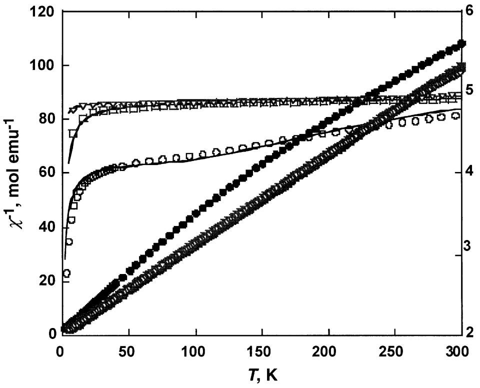

Figure 8. Reciprocal molar magnetic susceptibility χ^{-1} (closed) and moment, μ_{eff}, (open) as a function of temperature for α-[MnTClPPpy][HCBD]·PhMe (***α*-2Cl**) (circles), β-[MnTClPPpy][HCBD]·PhMe (***β*-2Cl**) (squares) and α-[MnTBrPP][HCBD]·PhMe (**3Br**) (triangles). Fit of the $\mu_{eff}(T)$ data to a zero-field-splitting with S = 2, $g = 1.99$ and $D = -1.45$ K (2.07 cm^{-1}) for α-[MnTClPPpy][HCBD]·PhMe (***α*-2Cl**) (solid line), fit of the $\mu_{eff}(T)$ data to the binuclear spin 2, ⁄1 2 expression (see text) for β-[MnTClPPpy][HCBD]·PhMe (***β*-2Cl**) (solid line) and fit of the $\mu_{eff}(T)$ data to a zero-field-splitting with S = 2, $g = 1.87$ and $D = 0.3$ K (0.2 cm^{-1}) for [MnTBrPPpy][HCBD]·2PhMe (**3Br**) (solid line).

In accord with the crystal structure, the magnetic properties of ***β*-2Clpy** were modeled to an S = ½, S = 2 dinuclear spin system using ($H = -2J\mathbf{S}_a \cdot \mathbf{S}_b$), Equation (2).[19b]

$$\chi = \frac{N\mu_B^2 g^2}{k_B(T-\theta)} \frac{10+35e(5J/T)}{4(2+3e(5J/T)} \qquad (2)$$

where N is Avogadro's number, μ_B is Bohr magneton, g is the Landé g value, k_B is the Boltzmann constant, and J is the exchange coupling constant. The solid curve in Figure 8 shows the best fit to the data between 70 and 300 K with $\theta = 2$ K, $g = 2.02$ and J/k_B of -90 K (-62 cm^{-1}). This J value is indicative of strong antiferromagnetic coupling between localized spin sites, while the positive θ indicates weaker interdimer coupling. Below 70 K the data is lower than the model prediction and may reflect to perturbations arising from D and TIP.

The susceptibility for **3Br** can be fit to a Curie–Weiss expression between 10 to 300 K with $\theta = -3.0$ K (Figure 8). θ for **3Br** is significantly lower than either [MnT*t*BuPP][HCBD] (-15 K)[5] or [MnOEP][HCBD] (67 K)[4] attributed to the low-spin density on the interior nitriles of [HCBD]$^{\bullet-}$.[5] The temperature dependence of **3Br** was similarly fit to Equation (1) with a $D = 0.3$ K (0.2 cm^{-1}), $g = 1.87$, and a TIP of 300 × 10^{-6} emu mol^{-1} (Figure 8). The genesis of low Landé g value is not well understood at this time; however, values as low as 1.82 have been reported for [Mn^{III}TPP]$^+$.[20] The low value of D reflect the slightly distorted octahedral coordination environment about Mn compared with the distorted square-planar environment of ***α*-2Cl**, and is lower than those observed to typical [Mn^{III}TPP]$^+$ complexes.[20]

Conclusion

The stoichiometric reaction of [Mn^{II}TXPPpy] (X = Cl, Br) with HCBD led to two distinct products ***α*-**, ***β*-2Clpy**, and **2Brpy** of [MnTXPPpy][HCBD] composition. On longer standing **3Br** of [MnTBrPP][HCBD] composition was formed. Although the structure of **2Brpy** has not been determined, based on the IR absorption spectra a structure related to the ***β*-2Clpy** is predicted. The $\tilde{\nu}_{CN}$ absorptions provide a signature of the differing bonding modes of [HCBD]^n ($n = 0$, 1 –, 2 –), Table 2. Furthermore, based on detailed examination the $\tilde{\nu}_{CN}$ absorptions of the α- and β-phases of **2Clpy** the two high frequency absorptions (i.e., 2185 ± 1 and 2170 ± 2 cm^{-1}) likely arise from unbound nitriles consistent with unbound [HCBD]$^{\bullet-}$ {e.g., [FeCp*$_2$][HCBD], 2185 (s) and 2168 cm^{-1}}. The low frequency nitrile absorption, however, exhibits a considerably wider range of absorptions and is likely due to coordination in the case of β-**2Clpy** or π-π interaction in ***α*-2Clpy.**

Table 2. Summary of the bonding modes of [HCBD]^n ($n = 0$, 1 –, 2 –) and their IR absorptions.

[HCBD]^n bonding mode	ν_{CN}				Ref.
π-HCBD^0	2247 (w)	2238 (m)	2211 (s)		
π-[HCBD]$^{\bullet-}$	2185 (s)	2168 (m)			[8]
trans-1,4-[HCBD]$^{\bullet-}$	2193 (s)	2150 (s)			[4]
trans-2,3-[HCBD]$^{\bullet-}$	2228 (m)	2212 (m)	2189 (w sh)		[5a]
σ-4-[HCBD]$^{\bullet-}$	2185 (m)	2170 (s)	2153 (m)		[5a]
π-[HCBD]$_2^{2-}$	2185 (s)	2170 (m)	2128 (m)		[5],[a]
π-[HCBD]$^{2-}$	2200 (m)	2152 (s)	2124 (w)		[a]
π-*iso*-[HCBD]$^{2-}$	2174 (s)	2158 (m)			[a]
trans-1,4-[HCBD]$^{2-}$	2181 (vs)	2107 (sh)	2141 (s)	2130 (sh)	
[$C_4(CN)_5O$]$^-$	2235 (w sh)	2226 (m)	2218 (s)	1557 (m)[a]	[a]

[a] This work. [b] ν_{CO}.

The [HCBD]$^{\bullet-}$ of ***α*-2Clpy** is unbound and has been characterized as the first [HCBD]$_2^{2-}$ dimer reported. Magnetic susceptibility experiments confirm the [HCBD]$_2^{2-}$ ground state to be a singlet, with preliminary ab initio calculations suggesting the singlet to triplet energy gap is ~65 kcal mol^{-1}.[16] The second product, ***β*-2Clpy**, consists of monodentate *exo*-bound [HCBD]$^{\bullet-}$ and was characterized as a binuclear S = ½, S = 2 system with strong antiferromagnetic coupling between spins. This is consistent with [MnOEP][HCBD], which also exhibits strong antiferromagnetic coupling. The β-phase is a clear intermediate between the unbound α-phase and the 1-D chain material. In contrast, **3Br** consists of the previously observed uniform 1-D ··· $D^+A^{\bullet-}D^+A^{\bullet-}$ ··· chains with Mn^{III} bridged by –2,3– (interior) bound [HCBD]$^{\bullet-}$, and confirms that this bonding motif leads to substantially weaker antiferromagnetic intrachain coupling with respect to –1,4– (exterior) bonding to

[HCBD]$^{\bullet -}$. The genesis of the two products appears to be competition of pyridine with [HCBD]$^{\bullet -}$ for Mn binding as evidenced from studies with excess [HCBD]$^{\bullet -}$ and substituted pyridine derivatives.

Experimental Section

Synthesis: All manipulations involving [HCBD]$^{\bullet -}$ were carried out under a nitrogen atmosphere using standard Schlenck techniques or in a vacuum atmospheres DriLab. Solvents used for the preparation of the [HCBD]$^{\bullet -}$ salts were predried and distilled from appropriate drying agents. H_2TXPP (X = Cl, Br) was prepared by a literature method.[22] [Mn^{III}TXPP]OAc was prepared from H_2TXPP and Mn(OAc)$_2\cdot 4H_2O$; the Mn(OAc)$_2\cdot 4H_2O$ was predissolved in *N*,*N*-dimethylformamide (DMF) and filtered before addition to the free-base porphyrin to remove impurities. [Mn^{III}TXPP]OAc was subsequently reduced to [Mn^{II}TXPPpy] [py = pyridine; X = Cl (**1Cl**), Br (**1Br**)] by NaBH$_4$ utilizing a literature method.[23] Substitution of pyridine with 2-methylpyridine (2-Mepy) and 2,6-dimethylpyridine was accomplished by reduction of [Mn^{III}TXPP]OAc in the presence of the substituted pyridines. HCBD was prepared by a literature method [3a] and was resublimed prior to use.

***α*-[MnTClPPpy][HCBD]·PhMe (*α*-2Clpy)**: [Mn^{II}TClPPpy] (**1Cl**, 35.3 mg, 0.036 mmol) was dissolved with stirring at room temperature in toluene (20 mL), and the dark-green solution was filtered through a medium glass-fritted funnel. A slight excess of HCBD (8.1 mg, 0.040 mmol) was dissolved in toluene (3.2 mL), and the red solution was similarly filtered. The above two solutions were mixed and allowed to stand 78 h in an inert-atmosphere glovebox. The resulting precipitate was collected by vacuum filtration and subsequently washed with fresh toluene (3 × 10 mL). TGA/MS indicated the presence of approximately one toluene and one pyridine per formula unit. Dark-green platelets suitable of X-ray diffraction were obtained by carefully layering the two filtered solutions, and ***α*-2Clpy** was harvested from the walls of the flask. IR (Nujol, NaCl, cm^{-1}): $\tilde{\nu}$CN 2185 (s), 2170 (m), 2128 (m).

***β*-[MnTClPPpy][HCBD]·PhMe (*β*-2Clpy)**: [Mn^{II}TClPPpy] (**1Cl**, 33.8 mg, 0.030 mmol) was dissolved with stirring at room temperature in toluene (10 mL), and the dark-green solution was filtered through a medium glass-fritted funnel. A slight excess of HCBD (7.8 mg, 0.050 mmol) was dissolved in toluene (3.0 mL), and the red solution was similarly filtered. These solutions were mixed at room temperature and allowed to stand 3 h in an inert-atmosphere glovebox. The resulting precipitate was collected by vacuum filtration and subsequently washed with fresh toluene (3 × 10 mL). The physical properties are identical to TGA/MS indicated the presence of approximately one toluene and one pyridine per formula unit. Green prisms suitable of X-ray diffraction were obtained from the original reaction mixture. Anal. calcd for ***β*-2Clpy·PhMe** $C_{66}H_{37}N_{11}MnCl_4$: C 67.13, H 3.16, N 13.05; found: C 66.95, H 3.11, N 12.88; IR (Nujol, NaCl, cm^{-1}): $\tilde{\nu}$CN 2185 (s), 2170 (m), 2153 (m); TGA/MS calcd for [MnTClPP][HCBD]py·PhMe, −py, −PhMe = 14.58%; found 14.52% at 114–306 °C ($m/z = 91$ amu, $m/z = 79$ amu).

[MnTBrPPpy][HCBD]·*x*PhMe (1 < *x* < 3) (2Brpy·): [Mn^{II}TBrPPpy] (**1Brpy**, 14.6 mg, 0.013 mmol) was dissolved with stirring at room temperature in toluene (20 mL), and the dark-green solution was filtered through a medium glass-fritted funnel. A slight excess of HCBD (3.5 mg, 0.017 mmol) was dissolved in toluene (5.0 mL), and the red solution was similarly filtered. The above two solutions were mixed and allowed to stand 4 h in an inert atmosphere glovebox. The resulting black-green precipitate was collected on a filter and washed with fresh toluene (3 × 10 mL). Attempts to obtain single crystals suitable of X-ray diffraction were unsuccessful. Anal. calcd for **2Brpy**·0.3PhMe, $C_{61.1}H_{31.4}Br_4MnN_{11}$: C 56.71, H 2.45, N 11.91; found: C 56.86, H 2.67, N 12.20; IR (Nujol, cm^{-1}): $\tilde{\nu}_{CN}$ 2185 (m), 2170 (s), 2153 (m); TGA/MS: calcd: for **2Brpy** = 19.0%; found 18.90% ($m/z = 91$ amu, $m/z = 79$ amu).

[MnTBrPP][HCBD]·2PhMe (3Br): The solution from **2Brpy** was allowed to stand for three weeks. Block crystals of **3Br** were isolated from the sides of the flask. IR (Nujol, cm^{-1}): $\tilde{\nu}_{CN}$ 2228 (m), 2212 (m), 2189 (w) (sh); TGA/MS = calcd toluene weight loss for **3Br**·2.10 PhMe: 14.01%; found 14.01% at 197 °C.

Physical methods: The 5 to 300 K magnetization was determined on a Quantum Design MPMS-5XL 5 T SQUID (sensitivity = 10^{-8} emu or 10^{-12} emu Oe^{-1} at 1 T) magnetometer, equipped with a reciprocating sample measurement system, and continuous low temperature control with enhanced thermometry features. Samples were loaded in gelatin capsules (gelcap) and mounted in plastic straws. For isofield dc measurements, the samples were zero-field cooled (following oscillation of the dc field to zero field), and data was collected upon warming. In addition to correcting for the diamagnetic contribution from the gelcap, core diamagnetic corrections of −478.7, −540.7, −162.0, −48.9, and -54.0×10^{-6} emu mol^{-1} were used for [Mn^{II}TClPP], [Mn^{II}TBrPP], HCBD, pyridine, and PhMe, respectively. The thermal properties were studied on a TA instruments model 2050 thermogravimetric analyzer (TGA) equipped with a electron spray mass spectrometer (ambient to 1000 °C) located in a vacuum atmospheres DriLab under nitrogen to study air and moisture sensitive samples. Samples were placed in an aluminum pan and heated at 20 °C min^{-1} under a continuous 10 mL min^{-1} nitrogen flow. IR spectra (600–4000 cm^{-1}) were obtained on a Bio-Rad FT-40 spectrophotometer. Elemental analyses were performed by Atlantic Microlabs, Norcross, GA.

X-ray structure determinations: Cell constants for ***α*-2Clpy** and orientation matrix for data collection were obtained from three oscillations exposed for 4.0 min at −135 °C on a Rigaku RAXIS-IV imaging plate area detector. The systematic absences indicate either of the monoclinic space groups P2$_1$ or $P2_1/n$. E-statistics favored the noncentrosymmetric alternative; this choice was confirmed by the stability of the refinement process. The structure was solved by direct methods and expanded using Fourier techniques. The nonhydrogen atoms were refined anisotropically. Hydrogen atoms were included, but not refined. The final cycle of full-matrix least-squares refinement was based on 9388 observed reflections [$I_o > 3.00\sigma(I)$] and 740 variable parameters and converged with unweighted and weighted agreement factors of $R = 0.069$ and $Rw = 0.069$. Crystallographic details for *α*-[Mn^{III}TClPPpy][HCBD]·PhMe (***α*-2Clpy**) are summarized in Table 3.

Cell constants and the orientation matrix for data collection for *β*-[Mn^{III}TClPPpy][HCBD]·PhMe (***β*-2Clpy**) were obtained from 10 images exposed for 30 s at 200 K on a Nonius Kappa CCD diffractometer. The systematic absences determine the space group $P2_1$. The structures was solved by direct methods and expanded using Fourier techniques using the SIR92[24] software package. Significant disorder was observed in the toluene solvate, subsequently the toluene was refined as a planar moiety. All other nonhydrogen atoms were refined anisotropically and hydrogen atoms were included, but not refined, using SHELX97-2[25] as part of the WinGX[26] graphics suite. The final cycle of full-matrix least-squares refinement for ***β*-2Clpy** was based on 9694 observed reflections [$I_o > 2.00\sigma(I)$] and 697 variable parameters and converged with unweighted and weighted agreement factors $R = 0.0672$ and $Rw = 0.1710$. Crystallographic details for ***β*-2Clpy** are summarized in Table 3.

Cell constants for **3Br** and an orientation matrix for the data collection were obtained by the standard method from 25 reflections at −80 °C on a CAD4 diffractometer. Systematic absences and subsequent least-squares refinement were used to determine the space group and uniquely define the space group as *P*. During data collection the intensities of several representative reflections were measured as a check on crystal stability, and there was no loss of intensity during data collection. Equivalent reflections were merged and only those for which $I_0 > 2\sigma(I)$ were included in the refinement, where $\alpha(F_o)^2$ is the standard deviation based on counting statistics. The weighing scheme used was: $[\alpha^2 F_o^2]^{-1}$. The structure was solved with the SIR92[24] program and refined based on the Patterson method within the SHELX-97 program.[25] The hydrogen atoms were included using the riding model where the H-atoms coordinates are re-idealized before each refinement cycle and "ride" on the atoms to which it is attached. Disorder in the [HCBD]$^{\bullet -}$ was observed, however, it could not be resolved within the data set. Crystallographic details for **3Br** are summarized in Table 3.

In an attempt to solve the structure of **3Cl**, the structure of a decomposition product of **3Cl**, namely, [Mn^{III}TClPP][$C_4(CN)_5O$]·2PhMe (**3Cl-O**) was unexpectedly determined. Crystals of **3Cl-O** suitable for X-ray diffraction studies were obtained from simple addition of HCBD and [Mn^{II}TClPPpy] in toluene with a drop of water added to the reaction mixture yielding dark-brown platelets. Cell constants and orientation matrix for data collection for **3Cl-O** were obtained from 45 images exposed for 10 s at 173 K on a

Table 3. Summary of the crystallographic details for α- (**α-2Clpy**) and β-[Mn^{III}TClPPpy][HCBD]·PhMe (**β-2Clpy**), [Mn^{III}TBrPP][HCBD]·2PhMe (**3Br**), and [Mn^{III}TClPP][$C_4(CN)_5O$]·2PhMe, (**3Cl-O**).

	α-2Cl	**β-2Cl**	**3Cl-O**	**3Br**
formula	$C_{66}H_{37}N_{11}MnCl_4$	$C_{66}H_{37}N_{11}MnCl_4$	$C_{67}H_{40}N_9MnOCl_4$	$C_{68}H_{40}Br_4MnN_{10}$
formula weight	1180.84	1180.84	1183.82	1371.68
space group	$P2_1/n$ (No. 14)	$P2_1$ (No. 4)	$P\bar{1}$ (No. 2)	$P\bar{1}$ (No. 2)
a [Å]	17.4463(3)	9.4277(3)	11.1255(2)	10.657(3)
b [Å]	15.6526(3)	20.9727(3)	13.8304(2)	10.832(2)
c [Å]	20.2121(3)	14.5913(4)	17.2040(2)	14.696(4)
α [°]	90	90	81.9800(4)	100.69(2)
β [°]	94.5090(9)	99.956(1)	85.3232(4)	78.65(2)
γ [°]	90	90	79. 8.9845(5)	118.33(2)
Z	4	2	2	1
V [Å^3]	5502.470(1)	2841.61(13)	2568.36(4)	1455.91(6)
ρ_{calcd}, g cm^{-3}	1.425	1.380	1.531	1.565
$R(F_o)$[a]	0.069	0.067	0.1047	0.078
$Rw(F_o)$[b]	0.069	0.176	0.2713	0.19
T [°C]	−135	−135	−100 (2)	−78
λ [Å]	0.710730	0.710730	0.710730	0.710730

[a] $R(F_o) = \Sigma w(|F_o| - |F_c|)/\Sigma|F_o^2|$. [b] $Rw(F_o) = \{\Sigma[w(F_o^2 - F_c^2]/\Sigma[w(F_o^2)^2]\}^{1/2}$.

Siemens P4 diffractometer equipped with a SMART/CCD detector. The centrosymmetric triclinic option was chosen and subsequently verified by the stability of the refinement process. The structure was solved by direct methods and expanded using Fourier techniques using the SHELXTL[25] software package. The nonhydrogen atoms were refined anisotropically and hydrogen atoms were included, but not refined using SHELXTL[25] graphics suite. Phenyl rings were treated as rigid planar bodies to conserve a reasonable data to parameter ratio. The final cycle of full-matrix least-squares refinement for **3Cl-O** was based on 7045 observed reflections ($I_o > 2.0\sigma$) and 620 variable parameters and converged with unweighted and weighted agreement factors $R = 0.1047$ and $Rw2 = 0.2713$. Crystallographic details for **3Cl-O** are summarized in Table 3.

X-ray crystal structure analysis: Crystallographic data (excluding structure factors) for the structures reported in this paper have been deposited with the Cambridge Crystallographic Data Centre as supplementary publication no. CCDC-102234 (**α-2Clpy**), -102235 (**β-2Clpy**), -102236 (**2Br**), and CCDC-102237 (**3Cl-O**). Copies of the data can be obtained free of charge on application to CCDC, 12 Union Road, Cambridge CB21EZ, UK (fax: (+44)1223-336-033; e-mail: deposit@ccdc.cam.ac.uk).

Acknowledgement

The authors gratefully acknowledge the support from the National Science Foundation (Grant No. CHE9320478).

---

[1] J. S. Miller, J. Calabrese, R. S. Mclean, A. J. Epstein, *Adv. Mater.* **1992**, *4*, 498.

[2] a) P. Zhou, B. Morin, A. J. Epstein, R. S. Mclean, J. S. Miller, *J. Appl. Phys.* **1993**, *73*, 6569; b) K. Griesar, M. Athanassopoulou, Z. Tomkowicz, M. Balanda, *Mol. Cryst. Liq. Cryst.* **1997**, *306*, 57; c) A. J. Epstein, C. M. Wynn, M. A. Girtu, W. B. Brinckerhoff, K.-i. Sugiura, J. S. Miller, *Mol. Cryst. Liq. Cryst.* **1997**, *305*, 321; d) M. A. Girtu, C. M. Wynn, K.-i. Sugiura, J. S. Miller, A. J. Epstein, *J. Appl. Phys.* **1997**, *81*, 4410; e) K. Griesar, M. A. Athanassopoulou, E. A. Bustamante, Z. Tomkowicz, A. J. Zaleski, W. Haase, *Adv. Mater.* **1997**, *9*, 45; f) K. Nagai, T. Iyoda, A. Fujishima, K. Hashimoto, *Chem. Lett.* **1996**, 591; g) W. B. Brinckerhoff, B. G. Morin, E. J. Brandon, J. S. Miller, A. J. Epstein, *J. Appl. Phys.* **1996**, *79*, 6147; h) J. S. Miller, A. J. Epstein, *Chem. Commun.* **1998**, 1319.

[3] a) O. W. Webster, *J. Am. Chem. Soc.* **1962**, *84*, 3370; b) M. D. Ward, *Electroanal. Chem.* **1989**, *16*, 182.

[4] J. S. Miller, C Vazquez, N. Jones, R. S. Mclean, A. J. Epstein, *J. Mater. Chem.* **1995**, *5*, 707.

[5] K.-i. Sugiura, A. M. Arif, D. R. Rittenberg, A. J. Epstein, J. S. Miller, *Chem. Eur. J.* **1997**, *3*, 138.

[6] a) T. Otsubo, Y. Kono, N. Hozo, H. Miyamoto, Y. Aso, F. Ogura, T. Tanaka, M. Sawada, *Bull. Chem. Soc. Jpn.* **1993**, *66*, 2033; b) G. Saito, T. Enoki, H. Inokuchi, H. Kumagai, C. Katayama, J. Tanaka, *Mol. Cryst. Liq. Cryst.* **1985**, *120*, 345; c) T. Sugimoto, M. Tsujii, E. Murahashi, H. Nakatsuji, J. Yamauchi, H. Fujita, Y. Kai, N. Hosoito, *Mol. Cryst. Liq. Cryst.* **1993**, *232*, 117; d) H. Yamochi, G. Saito, T. Sugano, M. Kinoshita, C. Katayama, J. Tanaka, *Chem. Lett.* **1986**, 1303; e) H. Yamochi, G. Saito, T. Sugano, M. Kinoshita, C. Katayama, J. Tanaka, *Synth. Meth.* **1987**, *19*, 533.

[7] J. S. Miller, J. Calabrese, D. Dixon, *J. Phys. Chem.* **1991**, *95*, 3139.

[8] J. S. Miller, J. Zhang, W. M. Reiff, *J. Am. Chem. Soc.* **1987**, *109*, 4584.

[9] **3Cl** can also be isolated from the reaction of excess HCBD, however, the purity of the sample could not be verified 2204 (w) and 2185 (m) cm^{-1}.

[10] E. J. Brandon, G. P. A. Yap, A. L. Rheingold, A. Arif, J. S. Miller, *Inorg. Chim. Acta* **1995**, *240*, 515.

[11] a) K. M. Kadish, F. Dsouza, A. Villard, M. Autret, E. V. Caemebecke, P. Bianco, A. Antonini, P. Tagliatesta, *Inorg. Chem.* **1994**, *33*, 5169; b) K. M. Kadish, M. Autret, Z. P. Ou, P. Tagliatesta, T. Boschi, V. Fares, *Inorg. Chem.* **1997**, *36*, 204; c) M. L. Yates, A. M. Arif, J. L. Manson, B. A. Kalm, B. M. Burkhart, J. S. Miller, *Inorg. Chem.* **1998**, *37*, 841.

[12] M. P. Byrn, C. J. Curtis, Y. Hsiou, S. I. Kahn, P. A. Sawin, S. K. Tendick, A. Terzis, C. E. Strouse, *J. Am. Chem. Soc.* **1993**, *115*, 9480.

[13] a) C. Katayama, M. Honda, H. Kumagai, J. Tanaka, G. Saito, H. Inokuchi, *Bull. Chem. Soc. Jpn.* **1985**, *58*, 2272; b) S. G. Clarkson, B. L. Lane, F. Basolo, *Inorg. Chem.* **1972**, *11*, 662.

[14] a) D. A. Clementea, A. Marzotto, *J. Mater. Chem.* **1996**, *6*, 941; b) M. Olmstead, G. Speier, C. Szobo, *J. Chem Soc. Chem. Commun.* **1994**, 541; c) J. S. Miller, D. O'Hare, A. Chakraborty, A. J. Epstein, *J. Am. Chem. Soc.* **1989**, *111*, 7853.

[15] See for example a) M. C. Grossel, S. C. Weston, *Chem. Mat.* **1996**, *8*, 977; b) A. Guirauden, I. Johannsen, P. Batail, C. Coulon, *Inorg. Chem.* **1993**, *32*, 2446; c) S. Z. Goldberg, P. Spivack, G. Stanley, R. Eisenberg, D. M. Braitsch, J. S. Miller, M. Abkowitz, *J. Am. Chem. Soc.* **1977**, *99*, 110; d) M. C. Grossel, S. C. Weston, *J. Phys. Org. Chem.* **1992**, *5*, 533.

[16] Calculations were performed using the SPARTAN v4.0 software package at the 621G** basis set single point energy. Starting geometry for the calculation was obtained from the crystals coordinates of **2Cl**. Calculations were carried out at unrestricted Hartree–Fock (UHF) level using the 6–31G** basis set in the SPARTAN4.0 program. Calculations were performed assuming both a singlet and triplet ground state to determine the lowest energy configuration.

[17] a) V. W. Day, B. R. Sults, E. L. Tasset, R. S. Marianelli, L. Boucher, *J. Inorg. Nucl. Chem. Lett.* **1975**, *11*, 505; b) B. Cheng, F. Cukiernik, P. Fries, J.-C. Marchon, W. R. Scheidt, *Inorg. Chem.* **1995**, *34*, 4627; c) R. Guildard, K. Perie, J-M. Barbe, D. J. Nurco, K. M. Smith, E. V. Caemebecke, K. M. Kadish, *Inorg. Chem.* **1998**, *37*, 973; d) J. T.

Landrum, K. Hatano, W. R. Scheidt, C. A. Reed, *J. Am. Chem. Soc.* **1980**, *102*, 6729; e) C. L. Hill, M. M. Williamson, *Inorg. Chem.* **1985**, *24*, 2834; f) E. B. Fleischer, *Acc. Chem. Res.* **1970**, *3*, 105; g) W. R. Scheidt, C. A. Reed, *Chem. Rev.* **1981**, *81*, 543; h) P. Turner, M. J. Gunter, T. W. Hambley, A. H. White, B. W. Skelton, *Inorg. Chem.* **1992**, *31*, 2297.

[18] a) E. J. Brandon, C. Kollmar, J. S. Miller, *J. Am. Chem. Soc.* **1998**, *120*, 1822; b) J. S. Miller, E. J. Brandon in *NATO ARW Supramolecular Engineering of Synthetic Metallic Materials*: *Conductors and Magnets* (Eds.: J. Veciana, C. Rovira, D. Amabilino), **1998**, *C518*, 197.

[19] O. Kahn, *Molecular Magnetism*, VCH, Weinheim, **1993**, p. 17.

[20] a) D. V. Behere, S. Mitra, *Inorg. Chem.* **1980**, *19*, 992; b) M. L. Yates, A. Arif, J. L. Manson, B. Kalm, B. M. Burkhart, J. S. Miller, *Inorg. Chem.* **1998**, *37*, 840; c) D. V. Behere, V. R. Marathe, S. Mitra, *Chem. Phys. Lett.* **1981**, *81*, 57; d) D. P. Goldberg, J. Telser, J. Krzstek, A. G. Montalban, L.-C. Brunel, A. G. M. Barret, B. M. Hoffman, *J. Am. Chem. Soc.* **1997**, *119*, 8722.

[21] R. L. Carlin, *Magnetochemistry*, Springer, Berlin, **1986**, p. 12.

[22] a) A. D. Alder, F. R. Longo, J. D. Finarelli, J. Goldmacher, J. Assour, L. Korsakoff, *J. Org. Chem.* **1967**, *32*, 476; b) L. R. Milgrom *Tetrahedron* **1983**, *39*, 3895; c) T. Ozawa, A. Hanaji, *Inorg. Chim. Acta* **1987**, *130*, 231.

[23] R. D. Jones, D. A. Summerville, F. Basolo, *J. Am. Chem. Soc.* **1978**, *100*, 446.

[24] SIR92, *A Program for Crystal Structure Solution*, A. Altomare, G. Cascarano, C. Giacovazzo, A. Guagliardi, *J. Appl. Crystallogr.* **1993**, *26*, 343.

[25] SHELX97–*2*, *Programs for Crystal Structure Analysis (Release 97–2)*, G. M. Sheldrick, Institüt für Anorganische Chemie der Universität, Tammanstrasse 4, 3400 Göttingen, Germany, **1998**.

[26] WinGX, *A Windows Program for Crystal Structure Analysis*, L. J. Farrugia, University of Glasgow, Glasgow, UK, **1998**.

Received: July 14, 1999 [F1916]